IEEE Open Journal of
Industry Applications

Received 6 May 2025; revised 26 July 2025; accepted 25 September 2025. Date of publication 1 October 2025;
date of current version 16 October 2025.

Digital Object Identifier 10.1109/OJIA.2025.3616287

Study of DC Arc Flash Phenomenon From 1000 V Lithium Ion Battery Systems

NICOLAUS JENNINGS [1], DAVID WETZ [1], ALEXANDER JOHNSTON [1], RICK LANGLEY [2], NANCY LAFLAIR [2], AND JOHN HEINZEL [3]

[1]University of Texas at Arlington, Pulsed Power & Energy Laboratory, Arlington, TX 760192 USA
[2]Electric Power Research Institute, Knoxville, TN 379323 USA
[3]NAVSE 05Z, Washington, DC 20374 USA

CORRESPONDING AUTHOR: DAVID WETZ (e-mail: wetz@uta.edu).

This work was supported in part by ONR under Grant N00014-21-1-2783 and in part by Army C5ISR Contract DOTC-17-01-INIT1218.

ABSTRACT Many civilian and defense applications are either considering or actively incorporating 1000 V electrochemical energy sources into their power systems for a multitude of uses. It is well known that lithium-ion batteries can introduce significant safety challenges, but the risk is most often worth the reward. In addition to the shock hazard that comes with high operational voltages, the potential danger to workers from arc flash hazard—intense heat, bright (blinding) light, and loud (deafening) sound—also exists, and it is not well documented from dc sources. As batteries become more attractive for use across industry, the risks posed by these sources drives a need to study the arc flash phenomena produced at application-relevant potentials. Consequently, the Electric Power Research Institute (EPRI) and the University of Texas at Arlington (UTA) have performed 91 arc flash experiments with battery sources at voltages roughly 1000 V_{dc}. Data collected from these experiments are the first comprehensive experimental analysis of dc arc flash phenomena from 1000 V lithium-ion battery systems, revealing previously unreported nonthermal hazards and overestimations from models typically employed. Two lithium-ion chemistries have been studied, Lithium Iron Phosphate (LFP) and Lithium Titanate (LTO). LFP modules studied previously at 540 V produced incident energies as high as 6.12 cal/cm^2 from an arc lasting 2.39 s with a gap distance of 0.25 in. At 908 V, the same LFPs exhibited upward of 4.48 cal/cm^2 from a 0.5 in gap distance tests that had to be manually cut off. LTOs at 730 V produced 2.16 cal/cm^2 for an arc lasting 0.88 s at a gap distance of 0.5 in. The light and sound intensity studied in some tests indicates the necessity for workers to use hearing and vision precautions. Models developed through this research and two relevant models from literature have been used to evaluate overestimations and their effectiveness at predicting the incident energy for arc flash events sourced from lithium-ion batteries.

INDEX TERMS Arc flash, electrochemical energy storage, incident energy, lithium-ion batteries, personal protective equipment.

I. INTRODUCTION

Usage of battery energy storage systems is on the rise as industrial, consumer, and military markets demand them. Industrial markets see the benefit dc systems provide for a source of backup power or prime power for machinery. In combination with ac generators, battery energy storage can be used to store excess energy that can be used later. With more people adopting electric cars or switching to off grid use comes the need to maintain and install these energy storage systems primarily and lithium-ion (Li-ion) battery technology is the most favorable candidate due to its high combined power and energy density. As the military marches forward with compacting existing systems, along with developing new technologies, energy storage is in lockstep with every decision. Current systems, such as naval platforms, employ energy storage for pulsed transient loads and for use as buffer for generators when they are transiently loaded. Energy storage already exists in these systems, but they take up considerable volume, especially when space is limited.

© 2025 The Authors. This work is licensed under a Creative Commons Attribution 4.0 License. For more information, see https://creativecommons.org/licenses/by/4.0/

Energy storage solutions can operate at voltages significant enough to cause concern for electric shock. Personal protective equipment (PPE) such as insulating gloves help prevent the possibility of electric shock when operating and performing maintenance. In addition to electric shock, a worker could experience an arc flash event from these sources and requisite PPE for this hazard must be worn. Arc flash events occur when two points of different voltage in a system ionize the air between them and start conducting through the plasma formed. This arc formation releases a blast of pressure, an intense blinding light, a loud deafening sound, and a great plume of heat that are all imparted directly on the face and the chest of any electrical worker. Blast pressure from an arc flash event can blow open electrical cabinet doors injuring workers and propelling them backward. The light produced can stun workers and potentially blind them, thus requiring them to wear eye protection. The loud sound produced by an arc can cause sudden hearing loss when in close proximity to the arc. Finally, the intense plume of heat, quantified as incident energy (IE), is the hazard most associated with arc flash fatalities. The heat produced can cause second degree burns or disfigure a person in a matter of seconds. Across all sectors of energy storage, worker safety is of the utmost priority and mitigating risks can be accomplished with PPE categorized through standardization.

Two standards that address the IE released by arc flash events are IEEE 1584 and NFPA 70E [1], [2]. IEEE 1584 focuses on IE from ac power systems and its scope does not cover single phase ac systems or dc systems [1]. NFPA 70E does address IE from ac and dc systems providing two methods of estimation that can be used to inform PPE [2]. One method estimates the IE by calculating the maximum power in the arc delivered by the dc system. The calculations this method uses overestimate actual IE values from empirical work and introduces scenarios where PPE is rated at a higher category than required. The equations used to estimate the IE from Informational Annex D.5.1 of NFPA 70E are shown in (1) and (2) [2]. An example analysis with them is shown for a 1000 V battery system to emphasize how severe estimations of IE can be.

A. EXAMPLE CASE STUDY

$$I_{arc} = 0.5 \times I_{bf} \tag{1}$$

$$IE_m = 0.01 \times V_{sys} \times I_{arc} \times T_{arc}/D^2. \tag{2}$$

Working with a vendor on IE calculations of a 1000 V Li-ion battery system, two studies looked at the inclusion and exclusion of over current protection devices (OCPDs). Without an OCPD, the bolted fault current I_{bf} was 4000 A and with it I_{bf} was reduced to 1400 A. Proceeding with system parameters in Table 1, the estimated IE IE_m, was found with (1) and (2) [2]. D is the "working distance" set at 45.7 cm and T_{arc} is the arc duration, chosen to be 2 s since that is estimated to be the time a worker would need to move a sufficient distance away from the arc to prevent further injury. While T_{arc} is set for the worst case of 2 s, the actual duration of the arc, especially with OCPDs present, will vary. In addition, one would also need to consider a function relating the distance of the worker away from the arc with respect to time to more accurately assess the IE on the worker. For the purpose of rating systems, the estimations in Table 1 present the worst-case scenario a worker may experience. The arc flash boundary is the distance away from the arc where the maximum IE is 1.2 cal/cm^2. With no consideration of a multiplier, IE was estimated to be 19.11 cal/cm^2 with no OCPD, and 6.70 cal/cm^2 with OCPD. In the first scenario, category 3 PPE is required, and category 2 is required for the second scenario. Then, if this arc fault were to take place inside of an enclosure, a maximum enclosure multiplier of 3 can be used to account for the amplification of IE from enclosures. Frequent application of an enclosure multiplier is used to conservatively estimate IE. This high multiplying factor often estimates IE at values that seem unrealistic given the battery system voltage and bolted fault current. Understanding if battery systems of this type can produce or partly obtain the estimated IE levels requires empirical work with similar systems.

TABLE 1. Example IE Analysis Parameter.

Parameter	Without OCPD	With OCPD
V_{sys}	1000 V	1000 V
I_{arc}	2000 A	700 A
T_{arc}	2 s	2 s
D	45.7 cm	45.7 cm
IE_m	19.14 cal/cm^2	6.70 cal/cm^2
$3 \times IE_m$	57.41 cal/cm^2	20.11 cal/cm^2

B. LITERATURE REVIEW

Arc flash studies of dc electrochemical energy storage have been performed using lead-acid stationary batteries [3], [4]. In [3], the energy storage system was a 125 V 1300 Ah battery with measured fault currents of 7850 A [3]. Hildreth et al. performed low voltage experiments at 125 V and recorded a maximum IE of 0.9 cal/cm^2. Then, after performing the NFPA 70E estimation method outlined above with their system parameters, the estimated IE was 10.3 cal/cm^2 with an enclosure multiplier of 1.6 [3]. Expanding upon previous work, Gaunce et al. studied a 125 V_{dc}, 400 Ah stationary battery under various environmental conditions [4]. Varying gap distances and humidity were studied with calorimeters placed from 38.1 cm (15 in) to as close as 15.24 cm (6 in). Upon compiling their test results into an empirical model, they overestimated the IE in 42 out of 70 experiments [4]. Measured IE from [3] and [4] shows that dc arc flash estimations can be overly conservative in determination of PPE.

Other works have utilized rectified sources to produce and study dc arcs [5], [6], [7], [8]. In [5], Weimann et al. looked at comparing experiments from [4], which were performed at a similar voltage to their battery supplied control system at their generator facility (125–130 V_{dc}). Sensitivity analysis

was performed on the gap distance between vertical copper bus bars and fault current. With the rectified source, fault currents were varied from 1.9 to 27.5 kA in increments of 5 kA. There, the authors found a vast overestimation of IE when utilizing (1) and (2) without an enclosure multiplier. Only one arc flash event, measuring 1.87 cal/cm^2, surpassed the arc flash boundary. This occurred at a 12.7 mm (0.5 in) gap with the highest bolted fault current. In [6], Schau utilized a Li-ion car battery configured in voltages from 48 to 480 Vdc and a rectified dc source at voltage up to 750 Vdc. This by the largest arrangement of physical lithium batteries available in the open literature. Schau was able to confirm across both source types at 400 V, 1.2 cal/cm^2 could be achieved. In [7], Cheng et al. performed 68 experiments at 600 V to evaluate arc flash IE for trolley overhead wires. The source utilized in their work was a 2 MVA 480 V_{ac} generator rectified to 600 V_{dc}. Most experiments were conducted inside an enclosure with different electrode configurations. Calorimeters placed 55.88 cm (22 in) away, in a vertical electrode arrangement, measured at most 1.1 cal/cm^2 for an arc lasting 100 ms with an arc current of 11.4 kA. Empirical equations were derived and found to need a multiplication factor to account for the enclosure and electrode arrangement when compared to open air results [7]. In [8], Gray et al. set out to measure IE from dc arcs ranging from 100 to 520 Vdc. The range of test covered arc fault currents of 2.7 to 10.9 kA. Instead of utilizing a metal enclosure, Gray opted for a ceramic enclosure to redirect the energy from the arc toward the calorimeters. Gray's findings show upward of 44 cal/cm^2 at a source potential 520 V with a 10.9 kA arc current for an arc that lasted 2 s. Comparing their work to the NFPA 70E method with no multiplying factor results in an IE estimation of 52.13 cal/cm^2. This finding reasonably estimates the IE, ensuring proper PPE for a worker.

Prior studies have primarily examined dc arc flash in low-voltage lead-acid battery systems [3], [4] or rectified dc sources [5], [6], [7], [8] ($\leq$750 V). However, these studies do not account for the distinct characteristics of lithium-ion batteries, which feature different impedance characteristics and arc sustainment behavior. Moreover, while arc flash modeling has been explored in ac systems direct application to lithium-ion dc sources remains unvalidated. This work fills this gap by presenting the first systematic analysis of dc arc flash hazards in lithium-ion battery systems up to 1000 V.

This work is among the first to cover arc flash experiments from batteries and characterize the potential hazards from Li-ion battery systems at these high potentials. The lack of 1000 V arc flash data from lithium-ion batteries drives the need to measure and estimate thermal and nonthermal injuries derived from arc flash events. These nonthermal events impact exposed electric workers hindering their vision and hearing. Two such events are studied in this work: sound pressure and light intensity. Sound pressure is closely related to an arc blast phenomenon where the initial expansion of air results in a loud sound and continues through the arc event. Being near and in the presence of an arc may damage the ear, leading to hearing loss. The bright light during the arc is much like that of arc welding and comparatively can be much brighter at distances of up to 3 m away like shown in [9]. The blinding light can temporarily stun the worker or at worse cause permanent blindness.

Working in collaboration, the Electric Power Research Institute (EPRI) in Knoxville, Tennessee, and the University of Texas at Arlington (UTA) Pulsed Power and Energy Lab (PPEL) have studied dc arc flash sourced from two Li-ion battery systems up to 924 V_{dc}. Experiments performed at EPRI were conducted using $Li_4Ti_5O_{12}$ (LTO) batteries at voltages ranging between 180 and 909 V. At UTA, experiments were conducted at 130 V up to 924 V using LFPs. Light intensity and sound pressure were recorded at UTA in addition to IE. This article is the first to cover dc arc flash phenomena from Li-ion batteries up to 1000 V and compare the IE measurements with IE models proposed in the literature. Results from this work will update or establish new guidance for arc flash PPE for workers performing maintenance on or around systems like those discussed. Current guidance uses a maximum power model that overestimates IE. Moreover, the assumption of these models is primarily based on rectified dc sources with no consideration for battery systems and the voltage drop that occurs in real storage. This work introduces the effect internal resistance has on reducing the arc conduction voltage and shows how estimations should be adjusted. Additional measurements of nonthermal injuries have been included to help inform standards on decisions for requiring PPE and establishing guidelines for electric workers.

In Section II, a Thevenin battery model is established within a simplified circuit that will be used later in IE estimation. In addition, the choice of electrode configuration and enclosure used will be discussed. Finally, coverage of the sensors and methods used to study arc flash related hazards are discussed in connection with an example experiment used throughout the article. In Section III, sensor measurements from arc flash experiments sourced with LFPs are discussed, including sound pressure and light intensity. In Section IV, measurements from arc flash experiments sourced with LTOs are discussed. In Section V, measured arc power is compared against three models of arc power that feed into Section VI's comparison of IE estimation.

II. TEST ENVIRONMENT

Studying the hazards present to workers requires a wide breadth of sensors to characterize each arc. Standards used to characterize PPE ratings for arc flash clothing were used to develop part of the sensor suite. ASTM F1989 [10] outlines a test method using copper calorimeters with thermocouples attached to the back of the device to ultimately measure the IE produced by the arc. Following the standard, K-type thermocouples were used. Light produced by the arc flash event likewise poses a hazard to workers and should be included to better assess PPE. Following work in [11], sensors like those in [12] were implemented to study light intensity produced in the arc events. Two Osram SFH 5711 sensors were used with two 4.2 optical density filters that reduced incident light

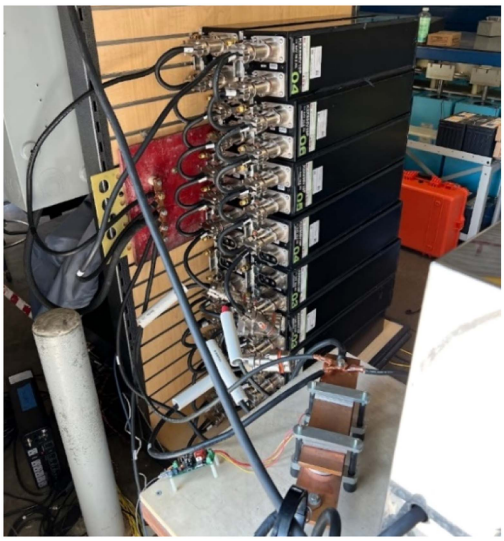


FIGURE 1. LFP battery stack arranged for a 160S/16P arc flash experiment with cables connecting to buswork. The solid state switch is composed of two silicon controlled rectifiers and is shown at the bottom middle of the figure sandwiched between two copper bus bars.

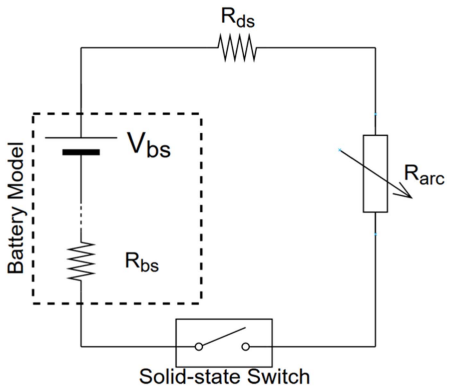


FIGURE 2. Arc flash test circuit incorporating Thevenin battery model, the resistance of the distribution network R_{ds}, nonlinear arc resistance R_{arc}, and solid-state switch are all shown as a simplified circuit.

onto the devices to a level below 100000 1×, which is as bright as direct sunlight. In [12], the sensors were placed much further away from the arc which ignores the immediate effect of proximity but all how the enclosure redirects light to the electric work increasing the overall intensity. These sensors were placed in front of the arc at a distance of 45.7 cm (18 in). Finally, sound pressure measurements were taken from a PCB Piezotronics 377C01 microphone PCB Piezotronics 426B03 preamplifier placed 61 cm (24 in). Light intensity measurements were fed into a National Instruments (NI) compact data acquisition (cDAQ) chassis card NI-9215. Sound pressure measurements were fed into the same cDAQ chassis into a NI-9230. Both metrics were sampled at 10 kHz. Both facilities studied IE released from arcs and all experiments performed at UTA captured sound and light measurements as well. Measurements of IE surpassed the minimum 70 Hz requirement in [10].

The first of two battery chemistries studied was the LFP type. The specific battery studied was a 64 V 10.2 Ah module composed of four parallel 20 series cells (20S/4P). Multiple modules were assembled in series/parallel to reach the desired voltage and capacity. Each of the modules was charged to 70 V prior to arc flash testing and the tests were performed in temperatures between 27 and 30 °C. A low voltage setup of those modules is shown in Fig. 1. The second chemistry studied are LTO batteries that are assembled in 44 V, 50 Ah modules made up of 16 cells in series. Modules were studied in series and parallel to achieve the desired voltage and capacity.

The Li-ion chemistries across facilities were studied at two gap distances. At UTA, 12.7 and 6.35 mm gaps were studied with the LFP chemistry allowing comparison with earlier work. EPRI included experiments at 6.35 mm while studying the LTOs. LFPs were studied in configurations from 40S/4P (130 V), 160S/16P (520 V), and 280S/8P (924 V). LTOs were studied in configurations of 64S/1P (180 V), 144S (405 V) up to 2P, 176S (500 V), 192S (550 V), 256S (730 V), 320S (909V).

The batteries used in these experiments were characterized and that data were applied to the IE model analysis to incorporate the correct source resistance. The source resistance of electrochemical energy storage largely affects the potential across the arc and how much energy can be delivered to sustain the arc. As the battery undergoes an arc fault scenario, the potential across the terminals drops due to internal resistance and leads to the arc extinguishing. Implementing the source resistance into calculations enables better arc power estimates.

A. BATTERY MODEL AND EQUIVALENT CIRCUIT

The batteries used in this work were originally purposed as the prime power for the high voltage chargers of a fast rise time capacitor bank. When computing the IE from arc flash events estimations of the system's resistance and the source resistance must be considered to study the arc power so a simple battery model, using its nominal and internal resistance has been studied. Battery characteristics will ultimately affect the slew of the fault current as the arc begins to form, which will impact the pressure formation of the arc and other phenomenon. Largely the rise time of the current will change the rate of the initial plasma expansion and ultimately expansion of air. The representative test circuit incorporating R_{bs}, V_{bs}, and R_{ds} is shown in Fig. 2, which also models the dynamic arc resistance and solid-state switch used to initiate the arc. A disconnect switch, not shown, is included for safety and to manually disconnect the arc. EPRI also included fuses in their arc flash testing. Of note, one LTO experiment was cut short because a fuse blew.

Two methods were explored to determine the internal resistance of the batteries used and create the Thevenin equivalent circuit. The first procedure followed an IEC 60896-21 [13] standard used to determine the short-circuit current of valve regulated lead acid batteries. Additional steps to this method

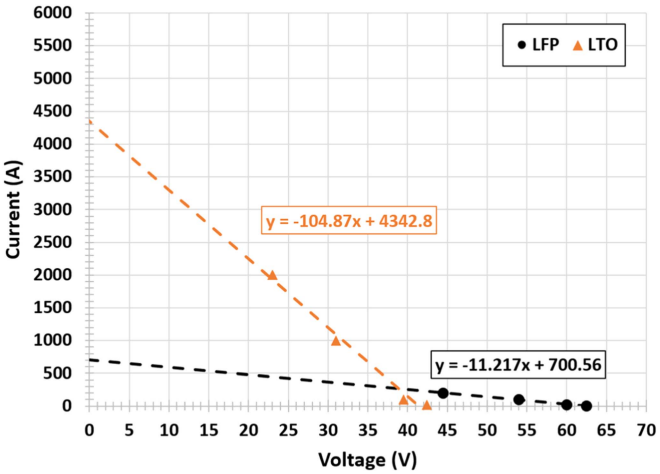


FIGURE 3. Line of best fit through various discharge currents with the conduction voltage at the constant current draw.



FIGURE 4. Inside UTA's enclosure looking through the opening. The walls of the enclosure are painted black. At the back of the enclosure is UTA's test fixture where the potential of the battery system feeds in and connects to bus work. The bus work connects to replaceable copper cubes that are at the bottom of a vertical electrode. Ceramic blockades are located above and behind the copper cubes.

were added based on [14] and improved short-circuit current estimation. Applying these methods to both Li-ion chemistries yielded Fig. 3 with lines of best fit through the discharge current and measured voltage drop, or conduction voltage, at the specific current draw. Back tracking these conduction voltages for higher and higher currents will trend toward the short circuit current for the battery technology. For LTOs, the estimated internal resistance per module was 9.5 mΩ and for LFPs the resistance per module was 58 mΩ.

The second method is more direct and is taken from experimental data. Since the electrodes are initially shorted with a fuse wire, the short-circuit current through the test circuit can be studied. Looking at the voltage and current data just before the arc forms, the initial voltage of the battery, short-circuit current, and bolted fault voltage can be found. Using this, the resistance of the battery was determined from the difference in voltage divided by the current. For the batteries at UTA, the internal resistance values remained the same, but this method showed that the LTO batteries at EPRI were closer to 7.3 mΩ per module.

B. ARC IN A BOX

A worker is likely to perform maintenance on a battery system connection in a metal enclosure. So, the goal was set to perform arc flash experiments inside of a metal enclosure allowing for the evaluation of these situations and the ability to study the multiplication of IE as opposed to an open-air arc. Following recommendations from IEEE 1584, low voltage switchgear has a listed maximum enclosure volume of 508 mm ×508 mm × 508 mm × 508 mm [1]. This size enclosure was built by EPRI and uses 12.7 mm diameter copper rods mounted vertically and centered in the box with an adjustable gap distance for the electrodes. UTA opted for smaller volume of 457 mm × 457 mm × 609.6 mm metal box used with vertical electrodes mounted at the back of the box capable of gap distance adjustment. UTA's enclosure is shown in Fig. 4, where two ceramic barriers were installed to limit the arc's ability to walk up the supporting bus keeping the arc attached on the replaceable electrodes. At the upper limits of voltages tested, these ceramic tiles were replaced almost every experiment. At both facilities, the interior is painted flat black, and the electrodes are replaced for each experiment.

The ceramic blockades performed as anticipated and constrained the arc to within the front section of the electrodes. The self-extinguishing times of the arc were likely improved by the barriers constraining the arc. This ultimately produces a worst-case scenario if an arc were to last for extended durations.

C. SENSOR BOARD

Thirteen copper calorimeters were placed in a large fiberglass board 45.7 cm (18 in) away from the arc location. The thermocouples connected to the back of each calorimeter was recorded for up to 30 seconds after the arc had extinguished. A FLIR thermal camera was also pointed to the side of the calorimeter board to back-up temperature measurements. The two light sensors were mounted on to the board facing the arc around 45.7 cm away. A neutral density filter holder was designed to mount to the light sensor and cover the sides of the device. The microphone sensor shown in the top middle of Fig. 5 is distanced 61 cm (24 in) away from the arc. Finally, high speed video from a Phantom camera recorded all arc flash experiments at 20 000 frames/s.

Finally, gap voltage and current data were recorded and used throughout discussions of hazards present to workers. A 160S/8P LFP experiment is shown in Fig. 6 and will be used as a demonstration of the data collected throughout this



FIGURE 5. LFP arc flash experiment from a 160S/16P 6.35 mm gap distance showing the high-speed video camera (top left of image), microphone (top middle), thermal imaging camera (middle left of image) pointed toward the enclosure at UTA, and the back side of the calorimeter board (middle).

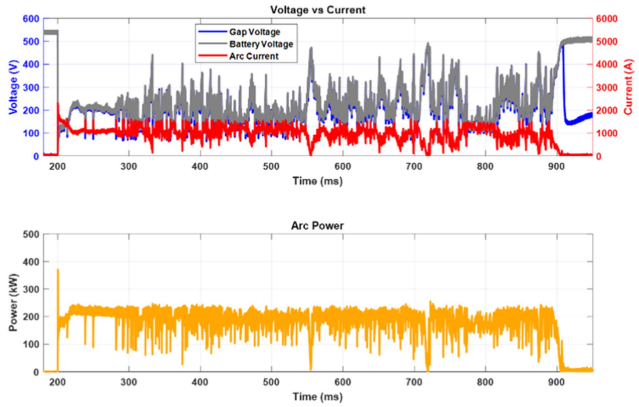


FIGURE 6. Arc voltage and arc current measured from a 160S/8P (536 V) experiment performed at 12.7 mm gap collected at UTA (top). Instantaneous arc power from the same experiment (below).

work. The experiment shown in Fig. 6 lasted 0.71 s and recorded a measured IE of 0.72 cal/cm^2. The voltage and current data from this experiment demonstrates nonlinear arc dynamics. At the formation of the arc, an initial fault current is established through the fuse wire until it vaporizes and an arc form between the electrodes. The stability of the arc from electrical data indicates a consistent arc length due in part because of the ceramic tiles limiting the arc's ability to walk up the supporting bus work. After a short period of time, the arc length expands and contracts as the arc moves across the copper cube electrodes. While the arc voltage and arc current

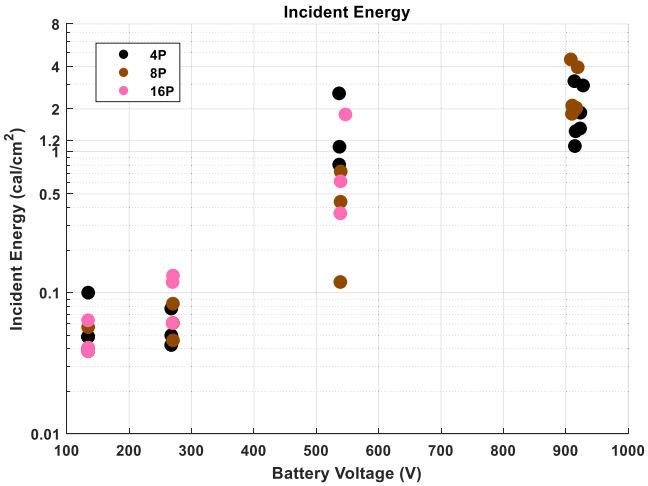


FIGURE 7. IE measurements from LFP arc flash experiments performed at 12.7 mm gap separation. A log scale is shown to provide clarity on the lower potential IE. The arc flash boundary of 1.2 cal/cm^2 is shown along with 4 cal/cm^2 (Category 1 PPE) and 8 cal/cm^2 (Category 2 PPE) [2].

vary wildly in the duration of the arc, instantaneous power envelopes arc dynamics staying bounded from formation of the arc to when it extinguishes. The average arc power from this experiment was 225.6 kW. At the tail end of the voltage curve, the solid-state switch opens, and the gap voltage records erroneous values, which were ignored in the analysis.

Moments where the arc power drops are attributed to the arc beginning to wane and a restrike following immediately. Overlaying captured data with high-speed video reiterates this showing at times the current would appear to fall to zero, but restriking through the ionized air re-igniting the arc. These restrikes were accompanied by light measurements indicating low light levels followed by a sudden increase in light. A collection of individual arc voltage and arc current measurements is too numerous to share in this form, but derived values from the data provide a good representation of the experiments.

III. LFP ARC FLASH EXPERIMENTS

The first of two Li-ion chemistries studied was using 64 V 10.2 Ah LFP batteries. Experiments at UTA were conducted at 40S, 80S, and 160S in string configurations of 4P, 8P, and 16P. At 280S, experiments were conducted in string configurations of 4P, 8P at 12.7 mm gap distance only.

A. IE

Measured IE from LFP batteries was the greatest among the chemistries experimented. Fig. 7 shows IE measurements from arc faults at a gap distance of 12.7 mm (0.5 in). From this, potentials below 270 V had small IE measurements (less than 0.2 cal/cm^2). For UTA at 536 V, IE showed propensity to exceed the arc flash boundary in numerous battery configurations. Those conducted in a 4P configuration had a peak IE measurement of 2.58 cal/cm^2 lasting 2.94 s. For an 8P configuration, the greatest IE measured was 0.72 cal/cm^2 and

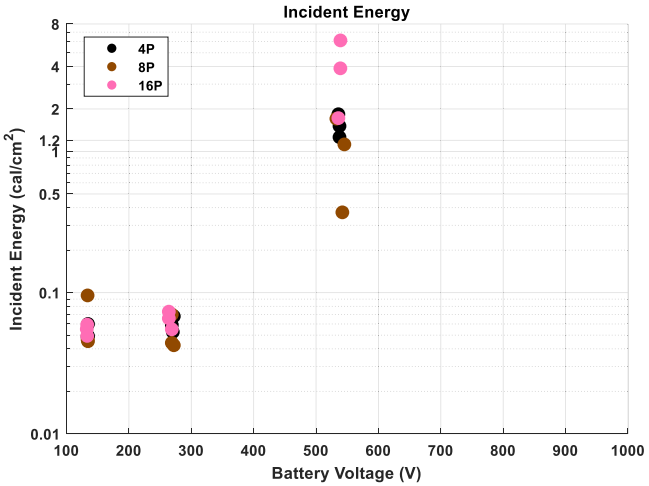


FIGURE 8. IE measurements from LFP arc flash experiments performed at 6.35 mm gap separation. A log scale is shown to provide clarity on the lower potential IE. The arc flash boundary of 1.2 cal/cm^2 is shown along with 4 cal/cm^2 (Category 1 PPE) and 8 cal/cm^2 (Category 2 PPE) [2].

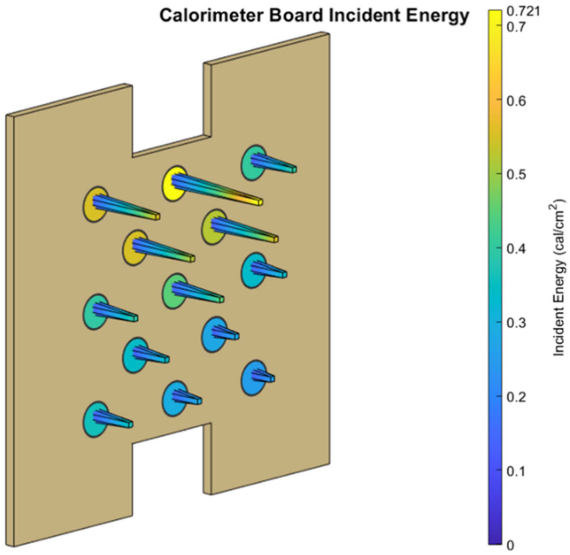


FIGURE 9. Plot of IE measurements across 13 calorimeters after an arc fault sourced from 160S/8P (536 V) at 12.7 mm gap distance. The orientation of the calorimeter board is facing the arc inside the enclosure.

for 16P it was 1.83 cal/cm^2. Only two experiments performed at this gap distance surpassed 1.2 cal/cm^2. At 536 V, the ability for an arc to sustain longer than a few hundred milliseconds in duration indicates a significant hazard at these potentials.

At 280S, the propensity of a severe arc flash event from LFP batteries is more than exemplified. Nearly all experiments at 4P exceeded the arc flash boundary and 4P experiments easily surpassed it. These experiments, unlike most at 160S, required the arc to be manually opened with the disconnect switch. With no chance the arc would self-extinguish the hazard risk regarding IE is met as to require PPE in these battery systems. While not shown, the first experiment to serve as an exploratory result at 280S, 16P with a 0.25 in gap distance ultimately led to a failure inside the batteries, ultimately causing a battery fire. A new set of LFP modules were utilized just for the 280S testing. Looking at the resistance during the initiation of the arc, these modules had higher ESR. This increased impedance lowers the potential supplied by the battery to the arc affecting its ability to sustain for any significant duration, ultimately reducing the IE released.

At UTA, all but one of the 160S arcs self-extinguished, with the one being manually opened at the disconnect switch. At a 12.7 mm (0.5 in) gap spacing the lowest parallel string count surpassing the 1.2 cal/cm^2 threshold demonstrates the worst-case scenario where an arc lasts two seconds and the worker is exposed to the arc while they move away. For each parallel string count, the average arc current is approximately 500 A, meaning that the 16P tests have an average current of 2000 A. The highest string counts will then have higher magnetic forces extending the arc length to a point where the potential of the battery is unable to support that arc length.

Fig. 8 shows experiments performed at a smaller gap distance of 6.35 mm. At this smaller gap distance, the effect of halving the distance between the electrodes halved led to a sharp increase in IE. At potentials less than 270 V_{dc}, IE from arc flash experiments did not surpass 0.1 cal/cm^2. At 536 V_{dc}, all LFP strings had produced measurable IE above 1.2 cal/cm^2. The greatest IE measured was from a 16P string with 6.12 cal/cm^2 lasting for 2.39 s. A second 16P experiment approached the 4 cal/cm^2 boundary of category 1 PPE. The greatest IE measured for 4P was 1.86 cal/cm^2 at 535.8 V, for 8P was 1.71 cal/cm^2 at 532.6 V, and for 16P it was 6.12 cal/cm^2 at 539.1 V.

Values in Figs. 7 and 8 represent the maximum value recorded across the entire array of calorimeters. When looking across the entire array, the density of IE across 13 calorimeters reveals the spread of energy coming from the enclosure. Fig. 9 uses the same 160S/8P experiment discussed in Section II showing the highest levels are found toward the top of the calorimeter board. The colors of the calorimeters correspond to the color bar on the right edge of the figure. The electrode geometry directs the energy toward the bottom of the box and does not directly expose the board to the plasma jets. The plume of heat then exits out of the front and toward the top of the enclosure rising with convection. The position of these calorimeters represents the chest of the exposed worker showing that IE released from these experiments affect the upper chest, neck, and face more than lower regions of the body. Correspondingly, category 1 PPE requires a layer of face covering whose ratings often exceed the category requirement (4 cal/cm^2). An improved sensor array of calorimeters would expand the board upwards and add calorimeters to the area representing the face and neck.

B. ARC DURATION

Arc duration contributes to the IE output from the arc fault and LFPs demonstrate the longest of the battery technologies studied. The recorded duration from experiments performed

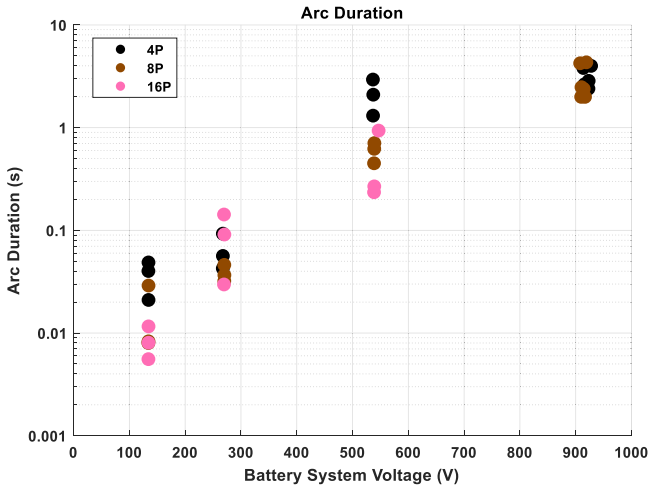


FIGURE 10. Duration of arc faults at a gap distance of 12.7 mm from LFP batteries. At potentials less 900 V, all experiments self-extinguished representing the limit of the arc flash. Beyond 900 V, all arc flash experiments had to be manually cut off.

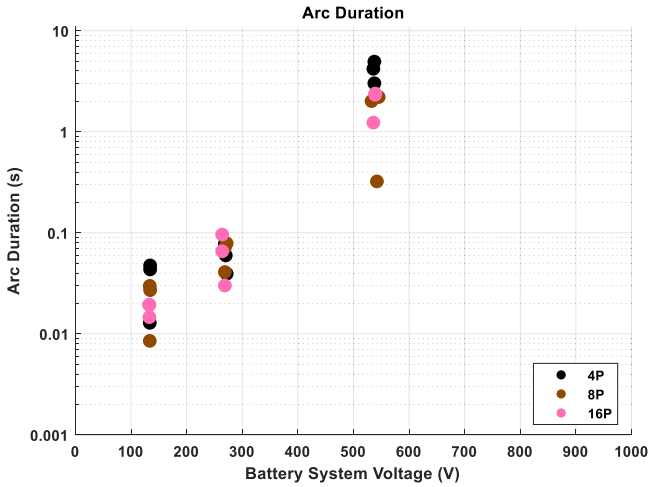


FIGURE 11. Duration of arc faults at a gap distance of 6.35 mm from LFP batteries.

at 12.7 mm in Fig. 10 show that potentials less than 270 V duration did not surpass 200 ms for all string configurations. At 536 V, durations for 4P lasted as long as 2.94 s, 0.71 s for 8P, and 0.936 s for 16P. The longer durations for lower string counts are expected because of the lower average arc current sourced. At higher potentials, this trend follows again with 4P consistently exceeding 1 s long durations. The highest potential test of 919 V, lasted for 4.32 s before being manually disconnected.

Along with the 12.7 mm gap experiments, arc durations at 6.35 mm were measured and follow similar trends from before. Fig. 11 demonstrates that for potentials less than 270 V, arc durations are less than 200 ms. However, average arc durations for 40S/16P (136 V) increased with the smaller gap distance. This is expected because the smaller gap distance means less potential is required to conduct across the gap and the extinction of the arc is driven by the lengthening of the arc. At 536 V, all string configuration tests had numerous tests exceeding 1 s in duration with the longest recorded experiment reaching 4.95 s for 4P, 2.21 s for 8P, and 2.39 s for 16P. Many of these tests were left to exceed 2 s to completely develop the arc and let them self-extinguish. Only one 536 V 16P experiment was stopped to preserve the integrity of the test equipment, specifically the highest IE one. Here, it is obvious that smaller gap distances lead to longer durations, which snowballs into higher incident energies measured. Like mentioned earlier, experiments at 280S had to be manually stopped because of the potential for the arc to damage the batteries and test equipment. For some calculations, researchers tend to use the duration of 2 s, however, in tight spaces the worker may be unable to move away from the arc within that time. The added value in these experiments allows a rough determination of whether the arc can be sustained for more than 2 s in these configurations. The ability for this level of potential will lead to arc flash events sustaining longer than 2 or even 4 s as shown here.

C. SOUND PRESSURE

Along with arc flash-rated clothing, other hazards present themselves to workers performing maintenance. Hearing precautions are recommended when performing maintenance on electrical systems. Characterizing the sound intensity from the arc fault phenomenon is associated with the arc blast scenario. The formation of the arc forces the air to rapidly expand and creates a blast and sound pressure wave. This blast wave is largely dependent on the rise time of the current and whether it sufficiently pushes enough air to cause a noticeable pressure rise further away. Of course, right near the arc, the largest pressure component will be available, but the lungs and ears are about 45.7 cm away, which will receive a much lower amplitude of pressure. Still the pressure component is necessary to show that these arc flash events sourced from battery systems are not capable of producing pressure that will cause lung or ear damage.

The loudest moments of the arc are at its formation and the relative sound intensity can decay as much as 9 dB throughout the duration of the arc. The maximum peak pressure taken from the microphone is used to show what type of transient can be expected from each arc event is shown in Fig. 12. The arc sound pressure demonstrated a positive trend with increasing voltage and increasing string count. The decrease in gap distance led to an increase in sound pressure for 4P configurations at 536 V. The loudest sound level measured was 121.5 dBA leading to a pressure rise of 16 Pa at 160S 16P.

D. LIGHT INTENSITY

The intense light released by these arcs measured at a distance of 45.7 cm away is graphed in Fig. 13 plotted on a log scale. At 130 V, light intensity did not vary with gap distance but increased with higher string counts. The brightest light measurement recorded at 130 V was nearly 16000 klx for 16P at both gap distances. Two events at 270 V demonstrated a

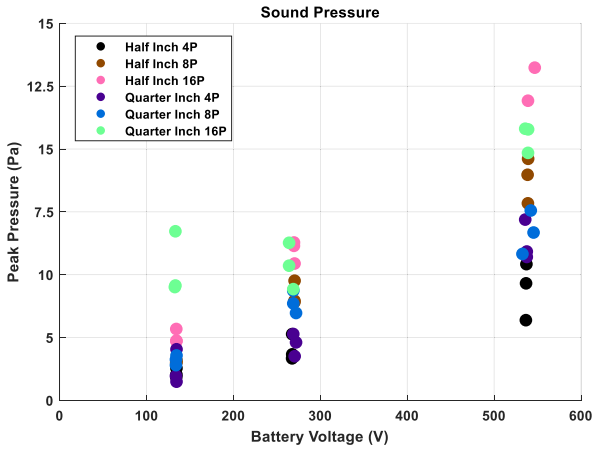


FIGURE 12. Peak sound pressure from arc faults from 12.7 and 6.35 mm gap distances studied at UTA.

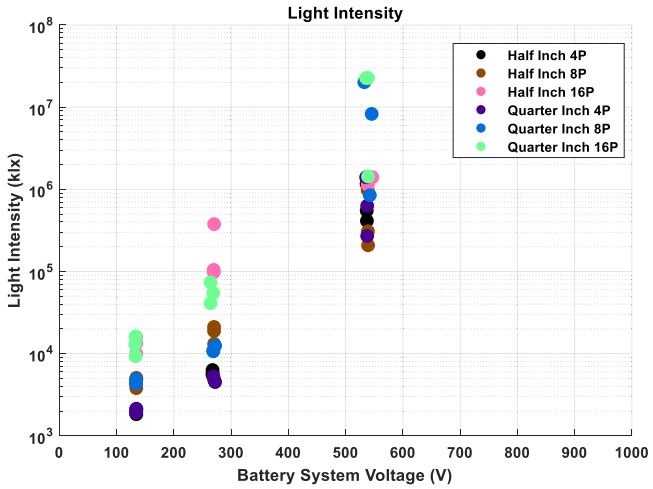


FIGURE 13. Arc light intensity taken from arc faults performed with LFP batteries. The intensity metric is the maximum recorded light intensity from two light sensors.

light intensity of 377000 klx and 105500 klx for 12.7 mm. At 536 V, the brightest experiment was 22612000 klx corresponding with a test that lasted for 1.23 s, had an IE of 1.72 cal/cm^2, peak sound level of 118.4 dBA. It is important to note that every light measurement did not saturated the light sensor. The total optical density per sensor was 4.2, so these filters proved sufficient in reducing the incident light to a level below 100000 l×.

While Fig. 13 shows the peak light intensity for each arc fault, the actual time scale reflects the dynamics of the arc event. Fig. 14 shows the example threaded throughout this article and demonstrates the initial formation of the arc and its corresponding light intensity. As the arc changes length throughout, moments of low light levels indicate restrikes in the arc. The brightest moment of the event occurs around 600 ms in the arc where the gap voltage floats around 120 V. Referring to the high-speed video and Fig. 14, this measurement

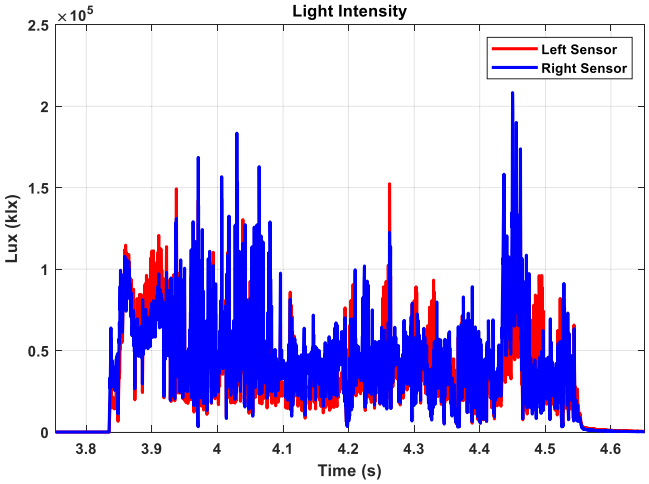


FIGURE 14. Example light intensity measurement from 160S/8P arc flash experiment at 12.7 mm gap distance.

of light intensity corresponds to the shortest arc length after the arc was formed.

Overall, the propensity of LFP batteries to produce significant IE to leave workers with severe burns is demonstrated by these experiments. The necessary PPE for the LFP batteries shown here is Category 1 (minimum 4 cal/cm^2) to Category 2 (minimum 8 cal/cm^2). The smaller gap distance experiments produced higher measured IE values due to the increase in arc duration across all arc currents measured. At 500 V in this system's configuration, the arc is more likely to sustain and develop into a damaging arc before extinguishing. At 900 V, the arc will sustain and continue until some electrical connection opens either in the battery or a switch in the circuit. Sound pressure measurements show a low change in pressure due to the slow rise time of the current in the system. Hearing protection should always be worn, but no special precautions such as lung or ear damage boundaries are shown. Light intensity is extremely severe considering the duration the arcs have shown to last. This alone prompts the need to wear auto darkening lens to limit the intensity of light that reaches the workers' eyes in the event of an arc flash.

IV. LTO ARC FLASH EXPERIMENTS

LTO experiments were performed at EPRI and included the use of fuses for value-added tests. Individual string measurements were recorded for each battery and IE for each test was measured. Two gap distances were studied to measure the effect a smaller gap distance provides for IE. At 12.7 mm, the battery was configured in a 1P and 2P configuration studying series counts of 64S. Additional series counts of 144S, 176S, 192S, 256S, and 320S were set up for 12.7 mm. At 6.35 mm, 64S, 96S, 144S, and 176S were studied for comparison at lower potentials.

A. IE

The IE released from LTOs did not surpass measured values of LFPs but they demonstrate risk above the arc flash boundary.

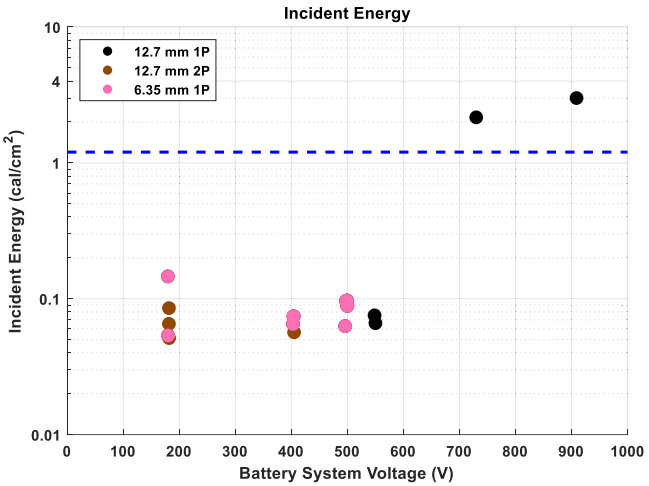


FIGURE 15. Measured IE from 1P and 2P LTO strings arc flash experiments at two gap distances.

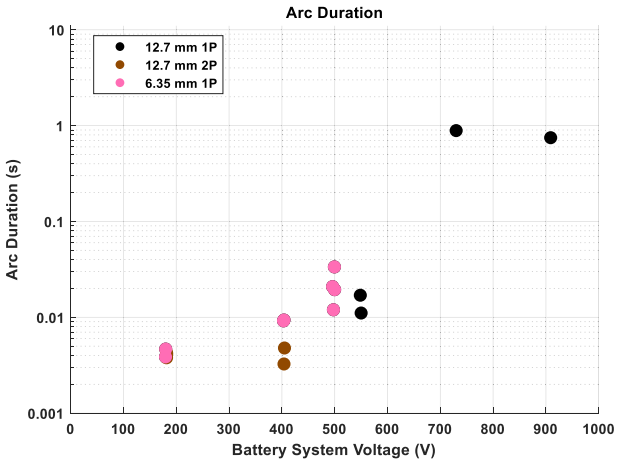


FIGURE 16. Arc duration versus battery system voltage across different string counts for an LTO battery.

While all of the experiments presented up until now were unfused, LTO experiments were fused to study their effects on arc durations. The summary of LTO experiments is shown in Fig. 15 with three configurations. Single string experiments at 12.7 mm demonstrated low IE levels for voltages below 548 V. At 730 V, the arc released 2.16 cal/cm^2 at a duration of 0.88 s. At 909 V, an arc lasting 0.75 s released an IE of 3.00 cal/cm^2 and the arc was extinguished when the 400 A fuse blew sustaining 6760000 A^{2}s. In a 2P configuration, the IE did not increase at the same potentials over the 1P experiments. A smaller gap distance at 6.35 mm did not increase the IE noticeably, even in a 1P configuration. The bolted fault current for 1P strings was between 4600 A for lower potentials and 5800 A for the highest potential. The 2P experiments nearly doubled this where 181 V had a bolted fault current of 7400 A and 404 V had 9500 A. When compared to LFP arc flash data, the IE produced was much lower from LTOs. The arc currents produced from LTOs drove the arc length too long ultimately to the point of arc extinction. In the case of electrochemical energy storage, these rapidly increasing arc lengths may not be supported because of the potential drop across the electrodes and source resistance. At 500 V, the IE measured from LTOs is far off from what was measured with LFPs. With the tipping point in LTOS found at 730 V with one experiment.

B. ARC DURATION

The duration of arcs sourced from LTOs in Fig. 16 stayed below 0.01 s for potentials less than 410 V. At 181 V, the 2P configurations had arcs lasting as long as 1P tests and the decrease in gap distance did not shown an increase in duration. At 400 V, the smaller gap distance did not increase the duration of the arc, even more, the higher string count experiments had arc durations not exceeding 0.005 s. At 500 V, the smaller gap distance increased the arc duration with a test lasting 0.017 s or slightly longer than one 60 Hz cycle. Like mentioned before, the two longest lasting experiments occurred at 730 V and 909 both in a 1P configuration.

In the LTO tests shown, arc durations greater than 800 ms produced IE near or above the arc flash boundary. Durations of an arc that did not sustain IE above 1.2 cal/cm^2 tended to be less than 200 ms. For LTOs, experiments with durations less than 40 ms measured insignificant amounts of IE. Above 800 ms, arc durations were great enough to sustain IE above the arc flash boundary. These experiments demonstrate that LTO batteries can produce IE requiring Category 1 PPE. While LTO batteries showed lower IE for a given voltage level, an investigation into the average arc power is necessary to determine what differences arise and how they can be used to estimate these hazards.

V. ARC POWER ANALYSIS

Like the instantaneous arc power shown back in Fig. 6, the average from each experiment is taken over the entire duration of the arc. This metric encapsulates the dynamics of the arc and is used in calculations for IE. IE estimations use relevant circuit parameters such as those shown in Fig. 2 in calculating arc power, which best represents the source used. Two common IE estimations will be compared to the average arc power from these experiments, and additional empirical results will be studied as well.

One estimation for IE is applied in NFPA 70E known as the max power model. This method applied by Doan [15], conservatively estimates that the source will deliver maximum power to the arc. Average arc current can be used to calculate the maximum power, but incorporating system parameters such as source resistance and distribution system resistance can specify and remove the dependence on arc current and its dynamics. Previously found battery and module resistance as well with distribution system resistance can be involved in the calculation of the maximum power P_{max}

$$P_{max} = \frac{V_{bs}^2}{4\,(R_{ds} + R_{bs})} \tag{3}$$

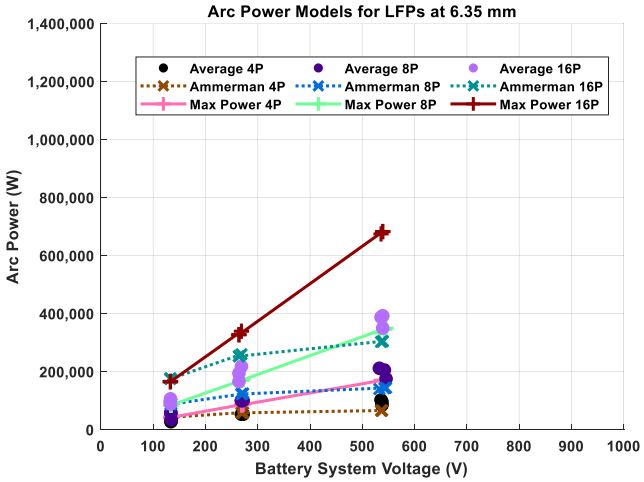


FIGURE 17. Comparison of measured arc power from LFPs studied at a gap distance of 6.35 mm to models proposed in the literature and standards. The dashed lines represent the calculated arc power from Ammerman's model and solid lines indicate maximum power calculated with Doan's method [15], [16].

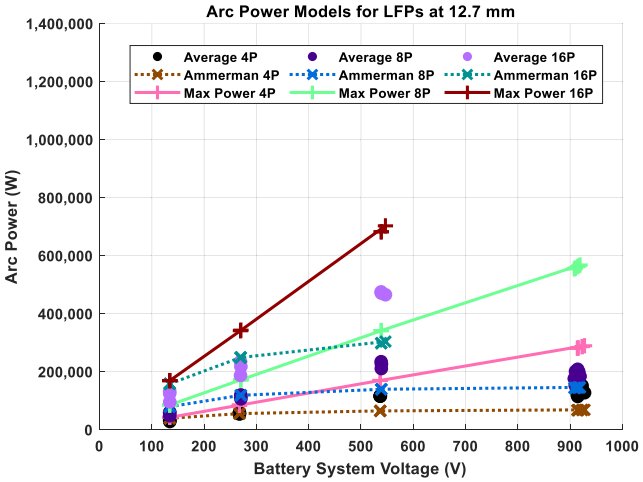


FIGURE 18. Comparison of measured arc power from LFPs studied at a gap distance of 12.7 mm to models proposed in the literature and standards. The dashed lines represent the calculated arc power from Ammerman's model and solid lines indicate maximum power calculated with Doan's method [15], [16].

where in (3), V_{bs} is the battery system voltage, R_{ds} is the equivalent resistance of the distribution system (3 mΩ for EPRI and 0.1 mΩ at UTA), and R_{bs} is the internal resistance of the battery. A second model derived empirically from the compilation of multiple dc arc flash studies derived by Ammerman [16] uses (4) and (5) solving for arc power which are manipulated form of the arc power model developed by Stokes and Oppenlander [17]. I_{arc} is found by iterating through (4) and (5) providing a close approximation of the arc power. Gap distance, g_{mm} in millimeters, is also included in this calculation as well as incorporating source and distribution system resistance

$$V_{arc} = \left(20 + 0.534{*}g_{mm}\right) I_{arc}^{0.12} \tag{4}$$

$$R_{arc} = \frac{\left(20 + 0.534{*}g_{mm}\right)}{I_{arc}^{0.88}}. \tag{5}$$

Application of these arc power models is shown in Figs. 17 and 18 for LFPs and Fig. 19 for LTOs. Trends for LFPs are similar at both gap distances and at all configurations so discussion for one configuration can be applied across all. Findings from the max power calculation for LFPs shows an upper bound for average arc power and its lower bound is near the Ammerman power. For voltages less than 270 V arc power follows the Ammerman model. This is expected given the much lower arc durations seen especially with higher string configurations. Above 270 V up to 924 V, arc power measures above Ammerman but consistently below max power corresponding with longer arc durations demonstrating the bounded nature of arc power.

Comparing the models calculated for LTO's arc power strikes similarities with models calculated for LFPs. Regardless of gap distance, the arc power was nearly identical for experiments at voltages below 500 V shown in Fig. 19. These

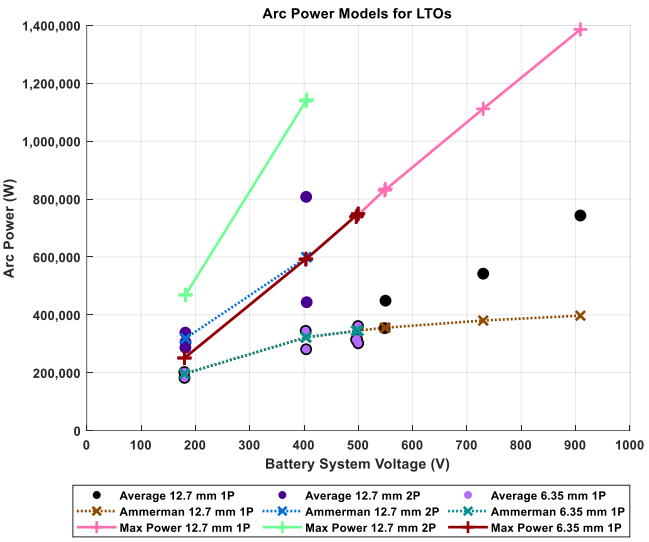


FIGURE 19. Comparison of measured arc power from LTOs studied at two gap distances of 12.7 and 6.35 mm against models proposed in the literature.

potentials studied with a single string showed close adherence to Ammerman with a similar explanation due to arc duration. At 730 V, arc power was above the calculated Ammerman power but below the max power.

To bridge the gap between the two facilities, test circuits, and remove strict dependence on the system parameters, a ratio of arc power is calculated. A new metric defined in (6) called battery bolted fault power or P_{bbf} is defined to establish this ratio. This ratio also serves to eliminate the dependence on electrical characteristics of the battery like ESR

$$P_{bbf} = V_{bs} I_{bbf} = \frac{V_{bs}^2}{(R_{ds} + R_{bs})}. \tag{6}$$

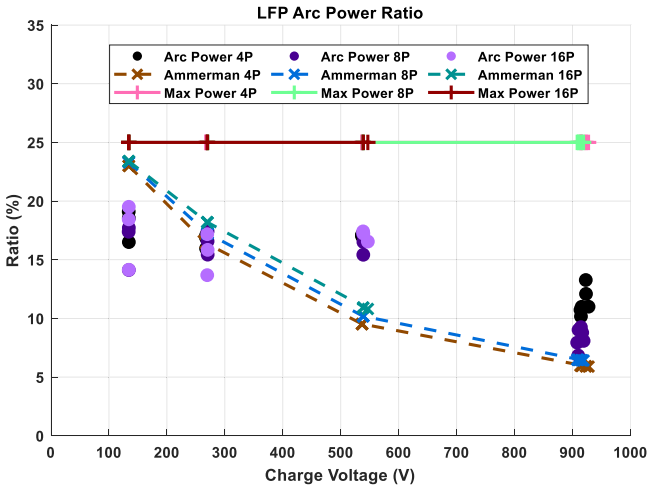


FIGURE 20. Arc power ratio from LFP experiments compared with arc power models. The solid circles represent average arc power ratio, dashed lines represent Ammerman model, and solid lines represent max power model.

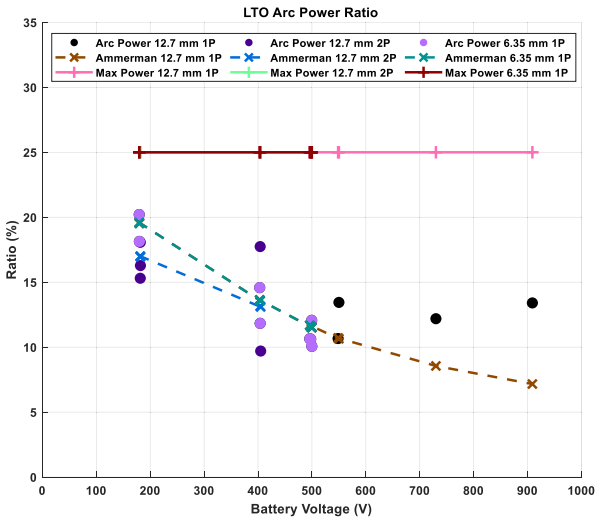


FIGURE 21. Arc power ratio from LTO experiments compared with Ammerman and max power models. Solid circles represent average arc power, dashed lines for Ammerman, and solid lines for max power model.

In (6), V_{bs} is the open circuit battery system voltage, I_{bbf} is the bolted fault current, R_{ds} is the distribution system resistance, and R_{bs} is the equivalent series resistance of the batteries. Meaning that (6) has a maximum of 25% because of the maximum power. This ratio also combines the string configuration's respective arc power into a value suitable for comparison. The calculated ratio is shown in Fig. 20 for all LFP experiments. For experiments up to 160S, a line through 16% provides a reasonable estimate for measured arc power ratio keeping half of the points above and the other half below the line. At 280S, the arc power ratio falls below this line most likely due to the difference in modules used. The LTO arc power ratio does not follow the same 16% found for LFPs. A reasonable estimate for LTOs would appear as 14% of P_{bbf} from Fig. 21. This ratio found for the battery chemistries will be applied in the next section to estimate IE.

VI. IE MODEL COMPARISON

IE models operate under the assumption that the arc power spreads uniformly in all directions in open air. In [1], the guide states that vertical electrode experiments conducted inside an enclosure measured greater IE than open-air tests as a result of the enclosure redirecting the heat toward opening where the calorimeters were. This explains why some apply a multiplication factor to IE models to enclosure-based calculations. With the arc power values provided by the models discussed previously, (7) can be applied to estimate the IE of an open-air arc

$$\mathrm{IE}\left(\frac{\mathrm{cal}}{\mathrm{cm}^2}\right) = \frac{P_{arc} * t_{arc}}{4\pi D^2} * 0.239 \frac{\mathrm{cal}}{\mathrm{J}}. \tag{7}$$

P_{arc} is the model arc power, t_{arc} is the arc duration, and D is the distance from the arc to the calorimeter board. While these experiments took place inside of an enclosure, these results will not include an enclosure multiplier for IE. The

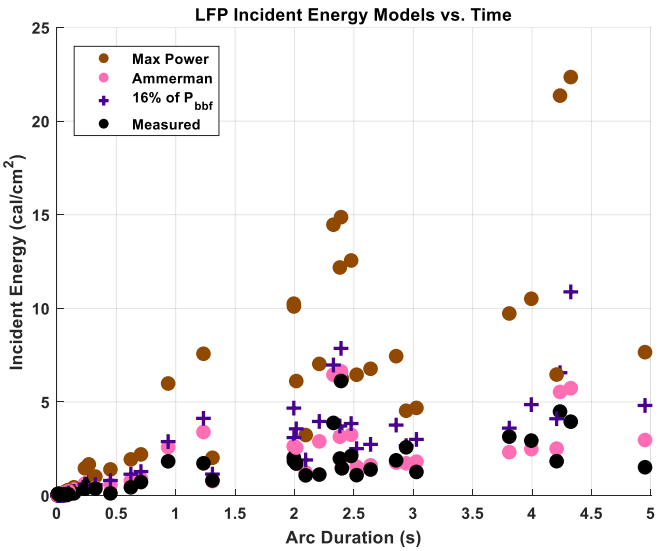


FIGURE 22. IE estimations for LFP experiments from models presented in text compared to measured values from all battery configurations. The measured values are shown in black, max power in brown, Ammerman in pink, and 16% of P_{bbf} in blue crosses.

IE estimations for LFPs are shown in Fig. 22 and LTOs in Fig. 23. For LFPs, the closet fitting model for these enclosure experiments was the Ammerman model. The next closest model was the battery bolted fault followed by max power. The max power model for the longest duration experiment (4.95 s) overestimates IE by nearly five times (up to 7.66 cal/cm^2) sufficient to require category 2 PPE.

The IE estimates for LTOs, in Fig. 23, demonstrate comparable results from LFPs with the Ammerman model being the closest to measured. For smaller arc durations, the estimates can underpredict the IE, but these durations do not represent significant IE released. The measured values for these experiments around 0.05 cal/cm^2 are measurements of noise

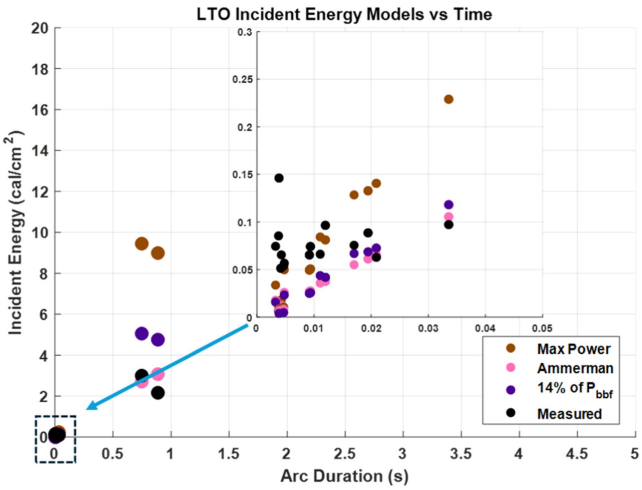


FIGURE 23. IE estimations for LTOs using relevant models presented in text compared to measured values at all battery configurations. The measured IE values are shown in black, max power in brown, Ammerman in pink, and 14% of P_{bbf} in blue.

and not actual IE findings. Since the maximum value of the thermocouple temperature was taken, spurious measurements are to blame. This does not mean that for short duration arcs, the thermocouples are incapable of measuring the change in temperature, but that the IE produced from the arc was not significant enough for an accurate measurement.

For the two experiments with durations greater than 0.5 s, the max power model overestimated a 0.89 s experiment by more than 4 times (up to 8.99 cal/cm^2) requiring category 2 PPE. This reiterates what much of the empirical data shows with the max power model [3], [4], [5], [6], [7], [8]. Finally, while the Ammerman model agrees well with the measured values of both chemistries studied, a few concerns are raised about its applicability.

First, (7) assumes the arc distributes its energy equally in all directions in open air. If the arc were surrounded by an enclosure, the enclosure would absorb and reflect the thermal radiation but the efficiency of this process is unknown to the author. Understanding the thermal effects of enclosure in arc flash has been studied for ac power systems but not for dc systems [18]. Thus, attempting to apply a multiplication factor to IE estimations is foolhardy when the assumption is that 100% of the arc energy is converted into thermal energy and 100% of the thermal energy is directed toward the worker. In fact, many times when going to reset an experiment, the higher IE experiments would leave the outer surface of the metal enclosure too hot to touch. Understanding how much the enclosure absorbs and how much it reflects would improve how relevant the enclosure is for multiplier factors in IE estimations. Second, Ammerman's model is a compilation of many arc flash studies present in the literature and is not purely derived a single work. Thus, any conclusions on its applicability must be considered. This also extends to (4) and (5) whose reliance on gap distance and development comes from series electrodes. Just nearly after the arc forms, raw data can be used to work backwards on the Stokes equations and then show when g_{mm} variable no longer agrees with the actual gap distance set in place.

VII. CONCLUSION

This study is the first to evaluate dc arc flash from Li-ion battery systems at potentials nearing 1000 V, providing the electrical safety community with empirical data that will help guide future experiments and develop new dc arc flash models. These data provide empirical evidence that many of the estimation models used today, overpredict the arc flash hazard. Over predicting the hazard can be very impactful, putting electrical workers in PPE that restricts them from operating more freely. The inclusion of sound and light intensity measurements expands the understanding of nonthermal arc flash risks, which have been largely absent from the literature. Two Li-ion battery technologies were used to source dc arc flash experiments. By using real battery energy storage systems in this work, the IE hazard risk is more readily apparent. Multiple experiments above 500 V surpassed 1.2 cal/cm^2 and sustained durations longer than 1 s. In evaluating PPE, light intensity values showed numerous magnitudes higher than a bright sunny day (100 klx). Compared to [9] at a closer distance, these findings represent severe incident light intensity on the workers eyes suggesting workers should employ vision protection. Sound pressure/intensity measurements demonstrated the repeated suggestion that workers should wear hearing protection when performing maintenance on these types of dc systems.

The experiments conducted in this article show that the IE models used today can overestimate the IE. The maximum power model was found to overestimate the IE in all the experiments performed. The Ammerman model was derived from arc flash data that is available in the literature and more closely aligns with the measured values presented in this article. This article considers the models discussed above and wraps them into a simple ratio. The basis of this ratio is defined in (6), called the battery bolted fault power P_{bbf}. The extrapolation of this ratio for all measured arc powers was determined to be 16% of P_{bbf}. Plugging P_{bbf} into (7), yielded estimations of IE near those measured empirically. This model was extracted from two different Li-ion chemistries and two similar, but different, test configurations at two different test facilities, lending to its credibility.

More recent work on IE estimation has proposed methods that outline ways to include real world effects from the arcs [19], [20] to better predict the incident energy. Namely, the effect of arc elongation or the growth of the arc length, and the erosion of the conductors. As the arc expands and contracts as portrayed in Fig. 6, the arc length subsequently changes throughout. High-speed video indicates numerous points where the arc contracts between the electrodes and expands out back toward the left and right edges of them numerous times. Modeling arc elongation can then be used to model the arc resistance throughout the duration to provide

a better estimation of arc power which can then be used in IE estimations. Conductor erosion is another real world effect whose consequence is an increase in arc lengths depending on the electrode configuration and current. The effect of conductor erosion in this work did not contribute significantly to an increase in arc length as the arc moved wildly across the electrodes and the duration with the applied currents did not significantly wane the conductors away to alter the arc lengths.

The work performed here suggests that not all arcs occurring within an enclosure, significantly amplify the IE imparted on the electrical worker. Therefore, it can be dangerous to apply those factors without experimental verification. Instead, the results collected here suggest that the multiplication factor should not exceed a unity value for this enclosure size. Because Ammerman's model was derived from the data collected in the literature, it should be applied cautiously until experimental data are collected under conditions representing those in which it is to be applied. These findings underscore a reason to step away from simple scaling factors solely based on the consideration of the arc occurring within an enclosure. These inaccuracies and overestimations can be addressed with consideration of the expanding arc length and the calculation or arc resistance as well as conductor erosion given an electrode configuration and arc current. Finally, the propensity for Li-ion batteries to produce dangerous arc flash hazards has been demonstrated at voltages as high as 924 V.

ACKNOWLEDGMENT

The opinions and findings here are those of the authors and may not reflect the views and opinions of ONR.

REFERENCES

[1] *IEEE Guide for Performing Arc-Flash Hazard Calculations*, IEEE Standard 1584-2018, Published Date: Nov. 11, 2018, © Copyright 2021 IEEE.

[2] *Standard for Electrical Safety in the Workplace*, NFPA Standard 70E, 2021 Edition, © National Fire Protection Association (NFPA), 2021.

[3] J. G. Hildreth and K. Feeney, "Arc flash hazards of 125 Vdc station battery systems," in *Proc. IEEE Power Energy Soc. Gen. Meeting*, Portland, OR, USA, 2018, pp. 1–5, doi: 10.1109/PESGM.2018.8586181.

[4] A. C. Gaunce et al., "Expanded DC arc flash model for 125V substation battery backup systems," in *Proc. IEEE/IAS 56th Ind. Commercial Power Syst. Tech. Conf.*, Las Vegas, NV, USA, 2020, pp. 1–9, doi: 10.1109/ICPS48389.2020.9176806.

[5] C. S. Weimann, R. J. Kerestes, and B. M. Grainger, "Comparative analysis of experimental DC arc flash results to industry estimation methods," *IEEE Open J. Ind. Appl.*, vol. 1, pp. 181–193, 2020, doi: 10.1109/OJIA.2020.3031768.

[6] H. Schau, "Risk parameters of DC fault arcs — Research work on DC arcs in LV systems," in *Proc. IEEE 12th Int. Conf. Live Maintenance*, Strasbourg, France, 2017, pp. 1–6, doi: 10.1109/ICOLIM.2017.7964116.

[7] K. S. Y. Cheng, C. Samson, and S. Cress, "DC arc-flash testing and analysis at 600 V," in *Proc. IEEE IAS Elect. Saf. Workshop*, Reno, NV, USA, 2020, pp. 1–6, doi: 10.1109/ESW42757.2020.9188330.

[8] K. Gray, S. Robert, and T. L. Gauthier, "Low voltage 100–500 Vdc arc flash testing," in *Proc. IEEE IAS Elect. Saf. Workshop*, Reno, NV, USA, 2020, pp. 1–7, doi: 10.1109/ESW42757.2020.9188336.

[9] W.-J. Lee, T. Gammon, Z. Zhang, B. Johnson, and S. Vogel, "IEEE\NFPA collaboration on Arc Flash Phenomena Research Project," *IEEE Power Energy Mag.*, vol. 10, no. 2, pp. 116–123, Mar./Apr. 2012, doi: 10.1109/MPE.2014.2322302.

[10] ASTM F1959/F1959-14E1, *Standard Test Method For Determining the Arc Rating of Materials for Clothing*, West Conshohocken, PA, USA: ASTM Int., 2014.

[11] W.-J. Lee, Z. Zhang, S.-H. Rau, T. Gammon, B. C. Johnson, and J. Beyreis, "Arc Flash light intensity measurement system design," *IEEE Trans. Ind. Appl.*, vol. 51, no. 5, pp. 4267–4274, Sep./Oct. 2015, doi: 10.1109/TIA.2015.2431638.

[12] S.-H. Rau, Z. Zhang, W.-J. Lee, and D. A. Dini, "Arc flash visible light intensity as viewed from human eyes," *IEEE Trans. Ind. Appl.*, vol. 53, no. 5, pp. 5068–5077, Sep./Oct. 2017, doi: 10.1109/TIA.2017.2715823.

[13] *Stationary Lead-Acid Batteries—Part 21: Valve Regulated Types—Methods of Test*, IEC Standard 60896-21, International Electrotechnical Commission, 2004.

[14] S. D. Gerner, P. D. Korinek, and T. E. Ruhlmann, *Calculated vs. Actual Short Circuit Currents for VRLA Batteries*. Horsham, PA, USA: C&D Battery Technologies. Retrieved: Jan. 26, 2023, [Online]. Available: https://www.sbsbattery.com/PDFs/VRLAshortCurrentsStorageBatterySystems.pdf

[15] D. R. Doan, "Arc flash calculations for exposures to DC systems," *IEEE Trans. Ind. Appl.*, vol. 46, no. 6, pp. 2299–2302, Nov./Dec. 2010, doi: 10.1109/TIA.2010.2070480.

[16] R. F. Ammerman, T. Gammon, P. K. Sen, and J. P. Nelson, "DC arc models and IE calculations," *IEEE Trans. Ind. Appl.*, vol. 46, no. 5, pp. 1810–1819, Sep./Oct. 2010.

[17] A. Stokes and W. Oppenlander, "Electric arcs in open air," *J. Phys. D, Appl. Phys.*, vol. 24, pp. 26–35, 1991.

[18] R. Wilkins, M. Allison, and M. Lang, "Improved method for arc flash hazard analysis," in *Proc. IEEE Ind. Commercial Power Syst. Tech.*, Clearwater Beach, FL, USA, 2004, pp. 55–62, doi: 10.1109/ICPS.2004.1314982.

[19] A. Marroquin and T. McKinch, "Methods for evaluating DC ARC-flash incident energy in battery energy storage systems," *IEEE Trans. Ind. Appl.*, vol. 60, no. 3, pp. 5150–5160, May/Jun. 2024, doi: 10.1109/TIA.2024.3353723.

[20] L. B. Gordon, "Modeling the dynamic behavior of DC arcs," *IEEE Trans. Ind. Appl.*, vol. 60, no. 1, pp. 1946–1955, Jan./Feb. 2024, doi: 10.1109/TIA.2023.3311780.